DOI: 10.1002/anie.200802278

Transition Alumina Phases

Mesostructured Forms of the Transition Phases η- and χ-Al_2O_3**

*Zhaorong Zhang and Thomas J. Pinnavaia**

Transition phases of alumina are metastable polymorphs of aluminum oxide formed through the thermal dehydration of aluminum trihydroxide (bayerite and gibbsite) and aluminum oxyhydroxide (boehmite) at temperatures between 230 and 1100 °C.[1] These oxides are used widely as catalyst components and adsorbents.[1–6] The chemical properties of a transition alumina phase are determined by a combination of surface acidity, which is directly related to the structure of the polymorph, the degree of surface hydroxylation, and textural properties, in particular, the surface area, pore volume, and pore-size distribution. η-Al_2O_3 is one of the most effective catalysts for the isomerization of unsaturated hydrocarbons owing to its exceptional surface acidity.[1,2,4,7–9] This transition phase has also been investigated extensively as a support for noble metals as catalysts for hydrodechlorination reactions.[10,11] Conventional η-Al_2O_3 prepared through the thermolysis of bayerite or pseudoboehmite typically contains only interparticle (textural) pores with a very broad pore-size distribution and has a relatively low surface area ($\leq 250\ m^2 g^{-1}$) after calcination at 500 °C.[1] χ-Al_2O_3 derived from the thermolysis of conventional gibbsite has a similarly low surface area.

It is generally recognized that the textural properties of alumina (and other metal oxides) can be improved substantially through the formation of a surfactant-templated mesostructure.[12–21] However, the mesostructured forms of alumina assembled from molecular precursors are generally comprised of atomically disordered (amorphous) framework walls that lack the stability and surface chemical characteristics of an atomically ordered (crystalline) transition alumina phase. Although an amorphous alumina phase can be transformed into the transition phase γ-Al_2O_3 at a temperature above 800 °C,[18,22] the calcination of a mesostructured amorphous alumina phase under such stringent thermal conditions inevitably destroys the mesostructure, even when the walls are stabilized by doping with rare-earth-metal ions.[18,23] A remarkable exception was reported recently for a dip-coated thin layer of amorphous alumina prepared through evaporation-induced supramolecular assembly.[24] This thin-layer form (< 1000 nm thickness) of mesostructured amorphous alumina maintained its mesostructured ordering upon thermal conversion into γ-Al_2O_3 at 900 °C. Spherical nanoparticles of amorphous mesostructured aluminum hydroxide, formed as an aerosol, were also transformed in part into mesostructured γ-alumina with a surface area of $134\ m^2 g^{-1}$ through calcination at 900 °C for short periods (10–30 min).[25] However, analogous thermolysis of bulk mesostructured forms of amorphous alumina has failed to afford a mesostructured transition alumina phase. Interfacial interactions with the supporting substrate almost certainly play a stabilizing role in the thermal transformation of an amorphous metal-oxide thin film into a crystalline thin-film mesostructure.[15] Surface energy may also facilitate the transformation of an amorphous alumina mesostructure in nanoparticle form into a more dense crystalline analogue.[25]

Previously, we demonstrated a general method for the formation of bulk quantities of mesostructured γ-Al_2O_3, denoted MSU-γ.[26,27] The key step in this method was the synthesis of a mesostructured boehmite mesophase denoted MSU-S/B with framework pores occupied by a nonionic surfactant.[28] Calcination of the mesophase at a temperature above 400 °C led to concomitant removal of the surfactant and transformation of the boehmitic walls into γ-Al_2O_3 with topochemical retention of the mesostructure. Owing to the substantial improvement in textural properties, MSU-γ derivatives with lathlike and scaffold particle morphologies were found to be highly effective supports for Co/Mo catalysts for the hydrodesulfurization of sulfides[21,29] and Re^{VII} oxide catalysts for the metathesis of olefins and their oxygen-containing derivatives.[30] An analogous surfactant-templating approach was adopted for the synthesis of high-surface-area mesostructured boehmite and γ-Al_2O_3 under microwave processing conditions.[31] Surfactants have also been used to mediate the particle morphology of boehmite and mesoporous γ-Al_2O_3 to include hollow tubes[32] and fibers,[33] although these latter derivatives were not mesostructured.

In continuation of our efforts to improve the textural properties of transition alumina phases through mesostructure formation, we report herein a facile approach to the synthesis of the first mesostructured transition alumina phases with walls comprised of crystalline η- and χ-alumina. These novel transition alumina phases, denoted MSU η-Al_2O_3 and MSU χ-Al_2O_3, respectively, were prepared through the assembly of mesostructured surfactant-encapsulated mesophases of bayerite and gibbsite from amorphous aluminum hydroxide by using an amine surfactant as the structure-templating porogen. Thermolysis of the bayerite or gibbsite mesophases above 400 °C afforded the surfactant-free mesostructured forms of η- and χ-alumina.

The colloidal amorphous aluminum hydroxide reagent used in the supramolecular assembly reaction was freshly prepared by base hydrolysis of aqueous $Al(NO_3)_3$ with ammonia solution at NH_4OH/Al^{3+} molar ratios of 3.0, 3.6, and 4.5. The NH_4OH/Al^{3+} ratio used in the formation of the colloidal hydroxide is important, as it determines the crystallinity of the mesostructured form of aluminum hydrox-

[*] Z. Zhang, Prof. T. J. Pinnavaia
Department of Chemistry, Michigan State University
East Lansing, MI 48824 (USA)
Fax: (+1) 517-432-1225
E-mail: pinnavaia@chemistry.msu.edu

[**] The partial support of this research by the National Science Foundation is gratefully acknowledged.

ide. The Keggin ion cluster $[Al_{13}O_4(OH)_{24}(H_2O)_{12}]^{7+}$, aluminate ion, or an aluminum alkoxide can be used in place of the aluminum salt; however, the use of $Al(NO_3)_3$ to produce the amorphous aluminum hydroxide reagent is more cost effective. Figure 1 A,B shows the small- and wide-angle XRD

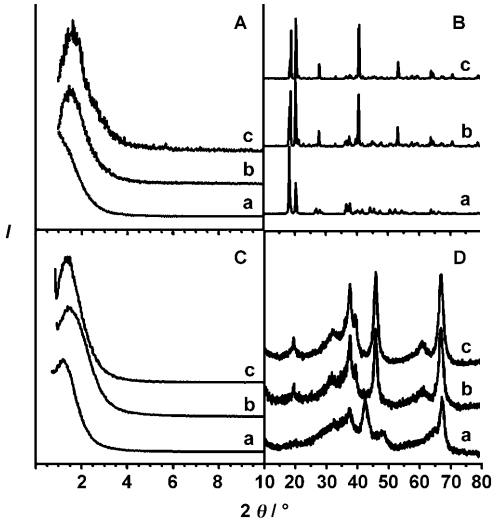

Figure 1. A) Small-angle and B) wide-angle XRD patterns of as-made mesostructured composites of a) gibbsite, b) bayerite admixed with some gibbsite, and c) bayerite. The composites were formed by the reaction at 100 °C of the surfactant tallow diamine with colloidal amorphous aluminum hydroxide precipitated from $Al(NO_3)_3$ at NH_4OH/Al^{3+} molar ratios of 3.0, 3.6, and 4.0, respectively. C) Small-angle and D) wide-angle XRD patterns of the mesostructured transition alumina phases formed by calcination at 500 °C of the corresponding as-made mesophases: a) MSU χ-Al_2O_3; b,c) MSU η-Al_2O_3.

patterns, respectively, of as-made gibbsite and bayerite mesophases assembled at 100 °C from freshly prepared aluminum hydroxide and tallow diamine (TDA, $C_{14-18}H_{29-37}NHCH(CH_3)CH_2NH_2$) as the structure-directing porogen. The presence of a single Bragg reflection in the small-angle XRD pattern of each mesophase is indicative of a wormhole framework structure[34] with a correlated pore–pore distance between framework pores. The multiple reflections found in the wide-angle XRD pattern of the mesophase prepared at an NH_4OH/Al^{3+} molar ratio of 3.0 (Figure 1 B, trace a) are characteristic of gibbsite (JCPDS card number 33-18), whereas the patterns for the products formed at NH_4OH/Al^{3+} molar ratios of 3.6 and 4.5 (Figure 1 B, traces b and c) indicate the predominant presence of bayerite (JCPDS card number 20-11). These results indicate that the crystallinity of the as-made mesophase walls is determined by the NH_4OH/Al^{3+} molar ratio used in the assembly reaction and that the encapsulated amine surfactant is compatible with framework walls made of gibbsite or bayerite.

Alkyl mono-, tri-, and tetraamine surfactants may be substituted for the diamine surfactant, provided that the amino group/aluminum molar ratio remains in the range 0.2–0.8. Alkyl amine porogens were found to be far more effective for encapsulation in mesostructured gibbsite and bayerite than block copolymers of polyethylene and poly(propylene oxide)s, perhaps as a result of more efficient hydrogen bonding of the amine porogens to the hydroxy groups of gibbsite and bayerite.

Depicted in Figure 1 C,D are the XRD patterns of the corresponding transition alumina phases obtained through the calcination at 500 °C of the as-made gibbsite and bayerite mesophases. The well-expressed single reflections shown in the small-angle patterns (Figure 1 C) indicate that the wormhole mesostructures were retained throughout the calcination process. Moreover, the wide-angle patterns clearly show that the gibbsite and bayerite framework walls were transformed into crystalline transition alumina phases. The calcined mesostructure derived from the gibbsite mesophase exhibited a wide-angle XRD pattern (Figure 1 D, trace a) characteristic of χ-Al_2O_3 (JCPDS card number 4-875), whereas the patterns for the mesostructures made from the bayerite mesophases (Figure 1, traces b and c) verify the presence of η-Al_2O_3 (JCPDS card number 04-0880). The transformation of mesostructured forms of gibbsite and bayerite into mesostructured χ-Al_2O_3 and η-Al_2O_3, respectively, parallels the conventional thermal transformation chemistry of these aluminum hydroxide phases.[1]

Figure 2 shows representative N_2-adsorption–desorption isotherms for MSU η-Al_2O_3 derived from the as-made TDA–bayerite mesostructure prepared at an NH_4OH/Al^{3+} ratio of 3.6. The linear uptake of nitrogen in the approximate range

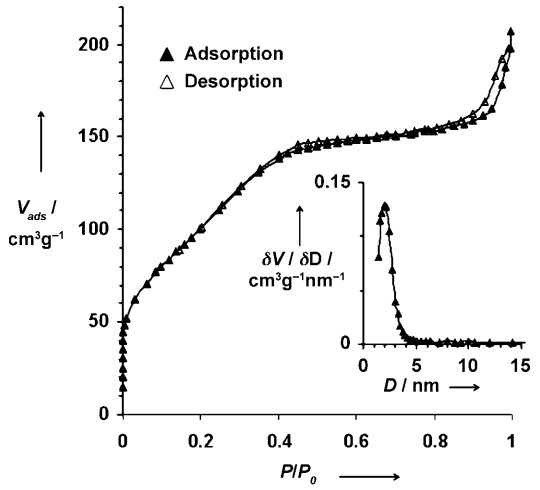

Figure 2. N_2-adsorption–desorption isotherms for MSU η-Al_2O_3 prepared through calcination of the as-made TDA–bayerite mesostructure prepared at an NH_4OH/Al^{3+} molar ratio of 3.6. The inset is the BJH pore-size distribution determined from the adsorption data.

$P/P_0 = 0.10$–0.40 is indicative of the presence of small framework mesopores, whereas the second uptake of nitrogen beyond $P/P_0 = 0.85$ suggests the presence of much larger textural mesopores formed through the aggregation of nanometric particles.[35] The Barrett–Joiner–Halenda (BJH) pore-size distribution derived from the adsorption isotherm (Figure 2, inset) is narrow for the framework pores and centered at a pore diameter of 2.1 nm.

Analogous N_2-adsorption–desorption isotherms and BJH pore-size distributions were found for the MSU η-Al_2O_3 and χ-Al_2O_3 compositions derived from the as-made mesostruc-

tures prepared at NH_4OH/Al^{3+} ratios of 3.0 and 4.5, respectively. Table 1 summarizes the textural properties of these representative mesostructured forms of transition alumina phases. Included in Table 1 are the pore–pore correlation distances (d_{001}) for each mesostructure.

Table 1: Properties of mesostructured MSU-η and MSU-χ alumina phases.

Mesophase	d_{100} [nm]	S_{BET}[a] [$m^2 g^{-1}$]	D[b] [nm]	Pore volume [$cm^{-3} g^{-1}$]
MSU η-Al_2O_3[c]	6.0	336	2.2	0.36
MSU η-Al_2O_3[d]	5.6	430	2.1	0.34
MSU χ-Al_2O_3	10.7	325	2.2	0.43

[a] Surface area determined from the Brunauer–Emmett–Teller equation. [b] Average BJH pore diameter derived from the adsorption isotherm. [c] Formed through calcination of an as-made TDA–bayerite mesophase prepared at an NH_4OH/Al^{3+} ratio of 4.5. [d] Formed through calcination of an as-made TDA–bayerite mesophase prepared at an NH_4OH/Al^{3+} ratio of 3.6.

Owing to mesostructure formation, the surface area of MSU η-Al_2O_3 is 336–430 $m^2 g^{-1}$. These values are 30–70% higher than the maximum value expected for a conventional η-Al_2O_3 phase formed through calcination of bulk bayerite at 500 °C.[1] Furthermore, the surface area of the MSU χ-Al_2O_3 phase described herein is 325 $m^2 g^{-1}$ or approximately 40% higher than the value observed for a conventional χ-Al_2O_3 phase derived from bulk gibbsite under the same conditions. A t-plot analysis of the adsorption isotherms indicated insignificant microporosity for both mesostructured oxides.

The morphology of the mesostructured aluminum hydroxide mesophases and the corresponding transition alumina mesophases were further characterized by transmission electron microscopy (TEM) and selected area electron diffraction (ED). Figure 3 shows representative micrographs of an as-made bayerite–TDA mesostructure and the corresponding MSU η-Al_2O_3 phase. The inset in Figure 3 is the ED pattern observed for the MSU η-Al_2O_3 mesophase. Unlike previously reported mesostructured boehmite and γ-alumina, both the TDA-containing bayerite mesostructure and the MSU η-Al_2O_3 transition alumina phase exhibit particle morphologies with well-defined crystallographic edges and angles. In contrast to the as-made TDA–bayerite mesostructure, the framework mesopores of which are filled by the surfactant, the surfactant-free MSU-η alumina exhibits open wormholelike mesopores formed through the intergrowth of lathlike nanocrystals that maintain the overall particle morphology of the precursor mesophase. The size of the mesopores between the nanocrystals is near 2.0 nm and thus consistent with the mean value obtained from the nitrogen-adsorption data (Figure 2, inset). The ED pattern of MSU η-Al_2O_3 is manifest as an array of diffuse diffraction spots and verifies that the framework walls of this composition are made by nanocrystal intergrowth. Qualitatively similar features were observed for the surfactant-encapsulated gibbsite mesophase and the corresponding mesostructured transition alumina phase MSU χ-Al_2O_3.

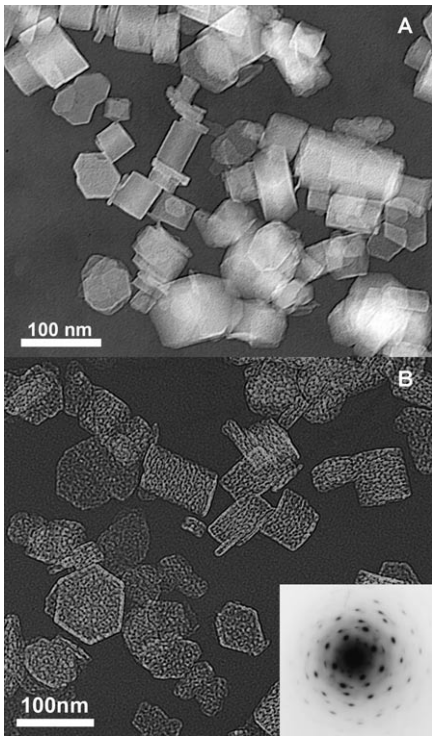

Figure 3. TEM images of A) the as-made bayerite–TDA mesophase prepared at an NH_4OH/Al^{3+} ratio of 4.0, and B) mesostructured MSU η-Al_2O_3 derived from the mesophase in (A) by calcination at 500 °C. The inset is the electron diffraction pattern of MSU η-Al_2O_3.

In view of the substantially improved textural properties of these mesostructured transition alumina phases, one may expect significant improvements in their performance in catalytic and adsorptive applications. Future studies will be devoted to the exploration of catalytic applications of these novel mesostructured forms of transition alumina.

Experimental Section

Amorphous aluminum hydroxide was prepared through the hydrolysis of $Al(NO_3)_3$ at NH_4OH/Al^{3+} molar ratios of 3.0, 3.6, and 4.5. The colloidal suspensions were centrifuged and washed with deionized water to remove the potentially explosive ammonium nitrate byproduct, and the $Al(OH)_3$ content was determined by weight loss on ignition at 600 °C. A portion of the centrifuged precipitate containing 0.02 mol of $Al(OH)_3$ was dispersed in deionized water (45 mL), and TDA (1.25 g) in ethanol (5 mL) was added. The resulting colloidal mixture was aged in a reciprocal shaking bath at 50 °C for 24 h and then heated at 100 °C for an additional 24 h. The resulting mesostructure was centrifuged, dried in air at room temperature for 24 h, and then dried at 100 °C for 6 h. The dried as-made TDA–gibbsite, TDA–bayerite, or mixed-phase TDA–gibbsite–bayerite mesostructures made at NH_4OH/Al^{3+} molar ratios of 3.0, 4.5, and 3.6, respectively, were calcined at 225 °C for 3 h and then at 500 °C for 4 h with a ramp rate of 2 °C min^{-1} to form the corresponding mesostructured MSU η-Al_2O_3 and χ-Al_2O_3 transition alumina phases. XRD patterns, TEM images, and ED patterns verified that the framework walls of both the mesostructured aluminum hydroxides and the calcined mesostructured transition alumina phases were crystalline. N_2-adsorption–desorption measurements provided evidence that mesostructured forms of transition alumina had substan-

tially improved surface areas and pore-size distributions relative to those of conventional forms of η- and χ-Al_2O_3.

Powder X-ray diffraction (XRD) patterns were obtained on a Rigaku Rotaflex X-ray diffractometer with $Cu_{K\alpha}$ radiation ($\lambda = 0.15405$ nm). Data were collected by using a continuous scan mode with a scan speed of $2\theta = 2°\,min^{-1}$. Isotherms for N_2 adsorption–desorption were analyzed with a Micromeritics ASAP 2010 or Tristar sorptometer at a temperature of 77 K. Samples were degassed under a vacuum of 10^{-5} Torr at 150 °C for 24 h prior to analysis. The pore-size distribution was calculated from the adsorption isotherms by using the BJH model. TEM images were obtained on a JEOL 100CX electron microscope equipped with a CeB_6 filament or a JEOL 2200FS field-emission microscope operating at an accelerating voltage of 200 kV. The specimen was prepared by sonicating the sample in ethanol for 10 min and then evaporating one drop of this suspension onto a 2.5 mm, 200 mesh carbon-coated grid.

Received: May 15, 2008
Revised: June 11, 2008
Published online: August 20, 2008

Keywords: aluminum oxide · bayerite · gibbsite · mesostructures · polymorphism

[1] C. Misra, *Industrial Alumina Chemicals*, ACS Monograph 184, American Chemical Society, Washington, DC, **1986**.
[2] H. Knözinger, P. Ratnasamy, *Catal. Rev. Sci. Eng.* **1978**, *17*, 31.
[3] V. H. J. De Beer, G. A. Somorjai, *Catal. Rev. Sci. Eng.* **1989**, *31*, 1.
[4] C. Morterra, G. Magnacca, *Catal. Today* **1996**, *27*, 497.
[5] A. L. Blumenfeld, J. J. Fripiat, *Top. Catal.* **1997**, *4*, 119.
[6] R. Prins, *Adv. Catal.* **2001**, *46*, 399.
[7] B. S. Gambhir, A. H. Weiss, *J. Catal.* **1973**, *31*, 243.
[8] A. K. Corado, H. Knozinger, H. D. Muller, *J. Catal.* **1975**, *37*, 68.
[9] K. Sohlberg, S. T. Pantelides, S. J. Pennycook, *J. Am. Chem. Soc.* **2001**, *123*, 26.
[10] K. A. Frankel, B. W. L. Jang, J. J. Spivey, G. W. Robert, *Appl. Catal. A* **2001**, *205*, 263.
[11] W. Sriwatanapongse, M. Reinhard, C. A. Klug, *Langmuir* **2006**, *22*, 4158.
[12] S. A. Bagshaw, T. J. Pinnavaia, *Angew. Chem.* **1996**, *108*, 1180; *Angew. Chem. Int. Ed. Engl.* **1996**, *35*, 1102.
[13] M. Yada, M. Machida, T. Kijima, *Chem. Commun.* **1996**, 769.
[14] F. J. P. Vaudry, S. Khodabandeh, M. E. Davis, *Chem. Mater.* **1996**, *8*, 1451.
[15] P. Yang, D. Zhao, D. I. Margolese, B. F. Chmelka, G. D. Stucky, *Nature* **1998**, *396*, 152.
[16] S. Cabrera, J. El Haskouri, J. Alamo, A. Beltran, D. Beltran, S. Mendioroz, M. D. Marcos, P. Amoros, *Adv. Mater.* **1999**, *11*, 379.
[17] S. Valange, J. L. Guth, F. Kolenda, S. Lacombe, Z. Gabelica, *Microporous Mesoporous Mater.* **2000**, *35–36*, 597.
[18] V. González-Peña, I. Diaz, C. Marquez-Alvarez, E. Sastre, J. Perez-Pariente, *Microporous Mesoporous Mater.* **2001**, *44–45*, 203.
[19] J. Cejka, *Appl. Catal. A* **2003**, *254*, 327.
[20] K. Niesz, P. Yang, G. A. Somorjai, *Chem. Commun.* **2005**, 1986.
[21] T. J. Pinnavaia, Z. R. Zhang, R. W. Hicks, *Stud. Surf. Sci. Catal.* **2005**, *156*, 1.
[22] Q. Liu, A. Wang, X. Wang, T. Zhang, *Chem. Mater.* **2006**, *18*, 5153.
[23] W. Z. Zhang, T. J. Pinnavaia, *Chem. Commun.* **1998**, 1185.
[24] M. Kuemmel, D. Grosso, C. Boissiere, B. Smarsly, T. Brezesinski, P. A. Albouy, H. Amenitsch, C. Sanchez, *Angew. Chem.* **2005**, *117*, 4665; *Angew. Chem. Int. Ed.* **2005**, *44*, 4589.
[25] C. Boissiere, L. Nicole, C. Gervais, F. Babonneau, M. Antonietti, H. Amenitsch, C. Sanchez, D. Grosso, *Chem. Mater.* **2006**, *18*, 5238.
[26] Z. R. Zhang, R. W. Hicks, T. R. Pauly, T. J. Pinnavaia, *J. Am. Chem. Soc.* **2002**, *124*, 1592.
[27] Z. R. Zhang, T. J. Pinnavaia, *J. Am. Chem. Soc.* **2002**, *124*, 12294.
[28] R. W. Hicks, T. J. Pinnavaia, *Chem. Mater.* **2003**, *15*, 78.
[29] R. W. Hicks, N. B. Castagnola, Z. R. Zhang, T. J. Pinnavaia, C. L. Marshall, *Appl. Catal. A* **2003**, *254*, 311.
[30] H. Balcar, R. Hamtil, N. Zilkova, Z. R. Zhang, T. J. Pinnavaia, J. Cejka, *Appl. Catal. A* **2007**, 320, 56.
[31] T. Z. Ren, Z. Y. Yuan, B. L. Su, *Langmuir* **2004**, *20*, 1531.
[32] H. C. Lee, H. J. Kim, S. H. Chung, K. H. Lee, H. C. Lee, J. S. Lee, *J. Am. Chem. Soc.* **2003**, *125*, 2882.
[33] H. Y. Zhu, X. P. Gao, D. Y. Song, Y. Q. Bai, S. P. Ringer, Z. Gao, Y. X. Xi, W. Martens, J. D. Riches, R. L. Frost, *J. Phys. Chem. B* **2004**, *108*, 4245.
[34] W. Zhang, T. R. Pauly, T. J. Pinnavaia, *Chem. Mater.* **1997**, *9*, 2491.
[35] F. Rouquerol, J. Rouquerol, K. Sing, *Adsorption by Powder and Porous Solids: Principles, Methodology and Applications*, Academic Press, London, **1999**.

